

Supporting Information

Enhancement of the Performance of Pd Nanoclusters Confined within Ultrathin Silica Layers for Formic Acid Oxidation

Jiefei Shan^a, Tang Zeng^a, Wei Wu^a, Yangyang Tan^a, Niancai Cheng^{a*}, Shichun Mu^{b*}

^a College of Materials Science and Engineering, Fuzhou University, Fuzhou, 350108 China.

^b State Key Laboratory of Advanced Technology for Materials Synthesis and Processing, Wuhan University of Technology, Wuhan, 430070, China.

E-mail: niancaicheng@fzu.edu.cn (N.C. Cheng); msc@whut.edu.cn (S.C. Mu).

*Corresponding author.

1. Experimental Section

1.1 Synthesis of Pd/NrGO@SiO₂:

We firstly prepared graphene oxide (GO) by a modified Hummers method.¹ For synthesis of the Pd/NrGO@SiO₂ catalysts, 100 ul 3-aminopropyl triethoxysilane (APTES) was firstly added into GO solution (0.3 mg/ml, 200 ml) with sonicating and stirred for 1 hour at 298 K. And then, 11.5ml K₂PdCl₄ (4 mg/ml) was added into the above dispersion solution with magnetic stirring. After magnetic stirring for 1 h, NaBH₄ (100.0 mM, 1.0 mL) was added into the above mixed solution with magnetic stirring, then washed three times with deionized water and freeze-dried. Finally, after redispersing of the sample into water solution, sodium hydrate (NaOH) was used to adjust PH of solution to 12 and 0.1 ml tetraethylorthosilicate (TEOS) was added dropwisely to the mixture. After stirring for another 1 hour, the sample were washed several times with water, and then freeze-dried. The as-prepared Pd/NrGO@SiO₂ was further treated at 300 °C in 10%H₂/90%N₂ atmosphere for 2 h. The Pd loading for Pd/rGO@pSiO₂ is 16 wt% by inductively coupled plasma mass spectrometer (ICP-MS).

1.2 Synthesis of Pd/NrGO

The synthesized method of Pd/NrGO is similar to the Pd/NrGO@SiO₂ without addition of TEOS. The Pd loading for Pd/NrGO is 22 wt% by Inductively Coupled Plasma Mass Spectrometer (ICP-MS).

1.3 Synthesis of Pd/rGO:

60 mg GO was well dispersed in 200 ml water with stirring and sonication, then 9.2 ml K_2PdCl_4 (4 mg/ml) was added to the mixture. After magnetic stirring for 1 h, 100 mg $NaBH_4$ was added into the above solution and washed several times with pure water, the resulting solution was also collected by filtering, dried and treated for 2 hours at $300^\circ C$ at 10% H_2 /90% N_2 atmosphere for 2 h. The Pd loading for Pd/rGO is 24 wt% by ICP-MS.

1.4 Materials characterization:

The morphology of the catalysts were performed using X-ray powder diffraction (XRD, Rigaku ULTIMA III), Atomic Force Microscope (AFM, Agilent 5500), and transmission electron microscopy (TEM, FEI TECNAL G2F2O). X-ray photoelectron spectroscopy (XPS) was taken on Thermo VG Scientific ESCALAB 250 spectrometer. Inductively Coupled Plasma Mass Spectrometer (ICP-MS) was performed on iCAP7000 (Thermo Fisher Scientific).

1.5 Electrochemical testing:

A standard three-electrode cell was applied to characterize electrochemical measurements using an Autolab electrochemistry station at room temperature. The working electrodes were achieved by deposition of 10 μ l uniform catalyst ink prepared by ultrasonically dispersing catalyst (4 mg) in 4 mL isopropanol and 40 μ L Nafion (5 wt. %). Platinum wire was used as a counter electrode while Ag/AgCl (sat. KCl) was used as a reference electrode.

Electrochemical active surface area (ECSA) measurements of all catalysts were carried out by measuring cyclic voltammetry (CV) curves in 0.5 M H₂SO₄. The ECSA was calculated from the peak of Pd(II) oxide reduction in CV by using the following equation:

$$\text{ECSA} = Q / [0.424 \times m_{(\text{Pd})}]$$

Where the Q represents the electric charges associated with the peak from reduction of Pd(II) oxide, which was calculated by area of the peak. Assuming 0.424 mC cm⁻² was required for the reduction of a Pd(II) oxide monolayer. In addition, m_(Pd) is the Pd loading on the electrode.

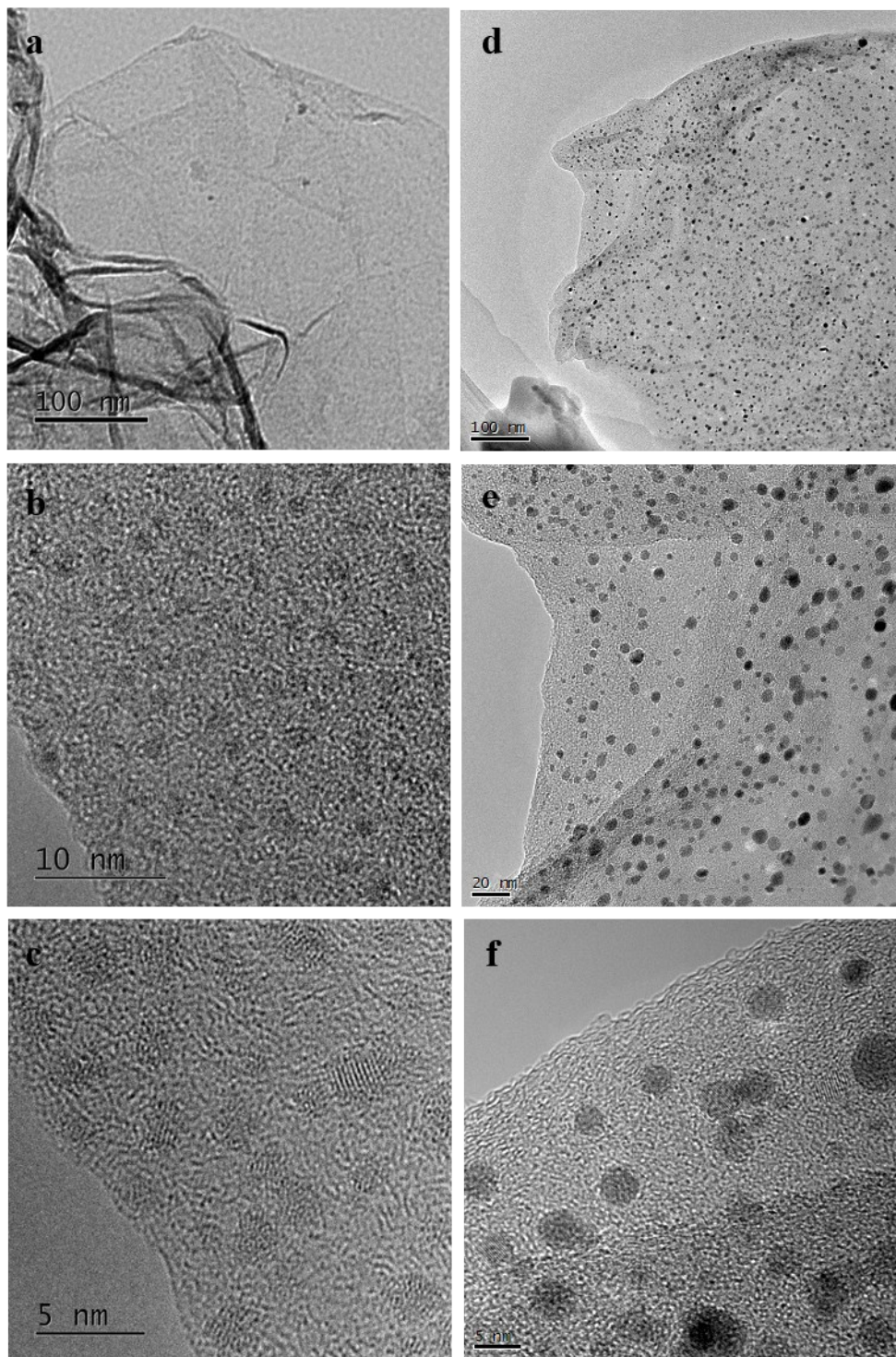


Figure S1. (a), (b) and (c) TEM images of Pd/NrGO sample before heating treatment. (d), (e) and (f) TEM images of Pd/rGO sample before heating treatment.

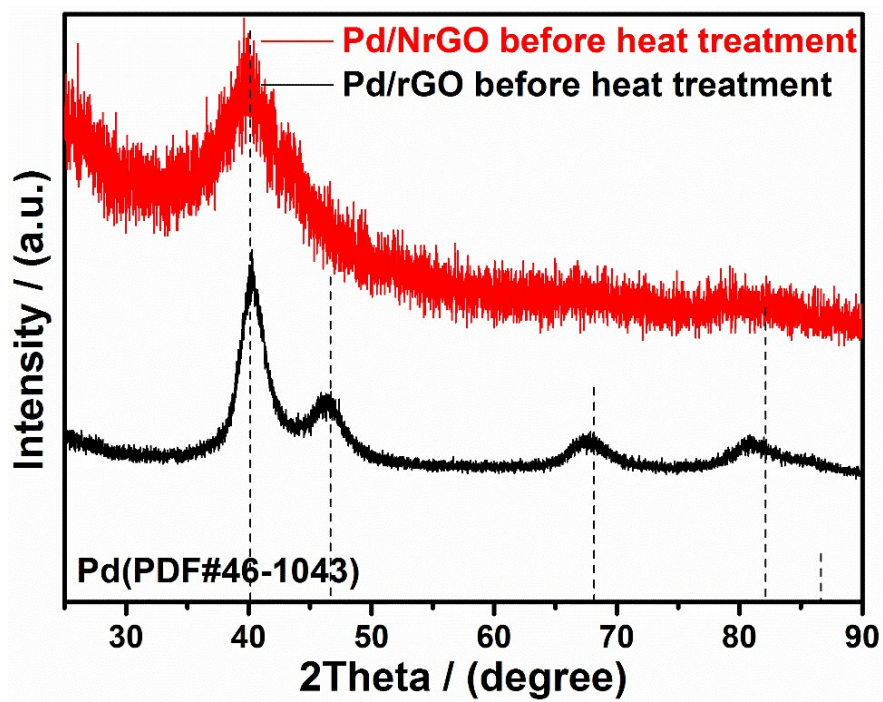


Figure S2. XRD patterns for Pd/rGO, Pd/NrGO before heat treatment.

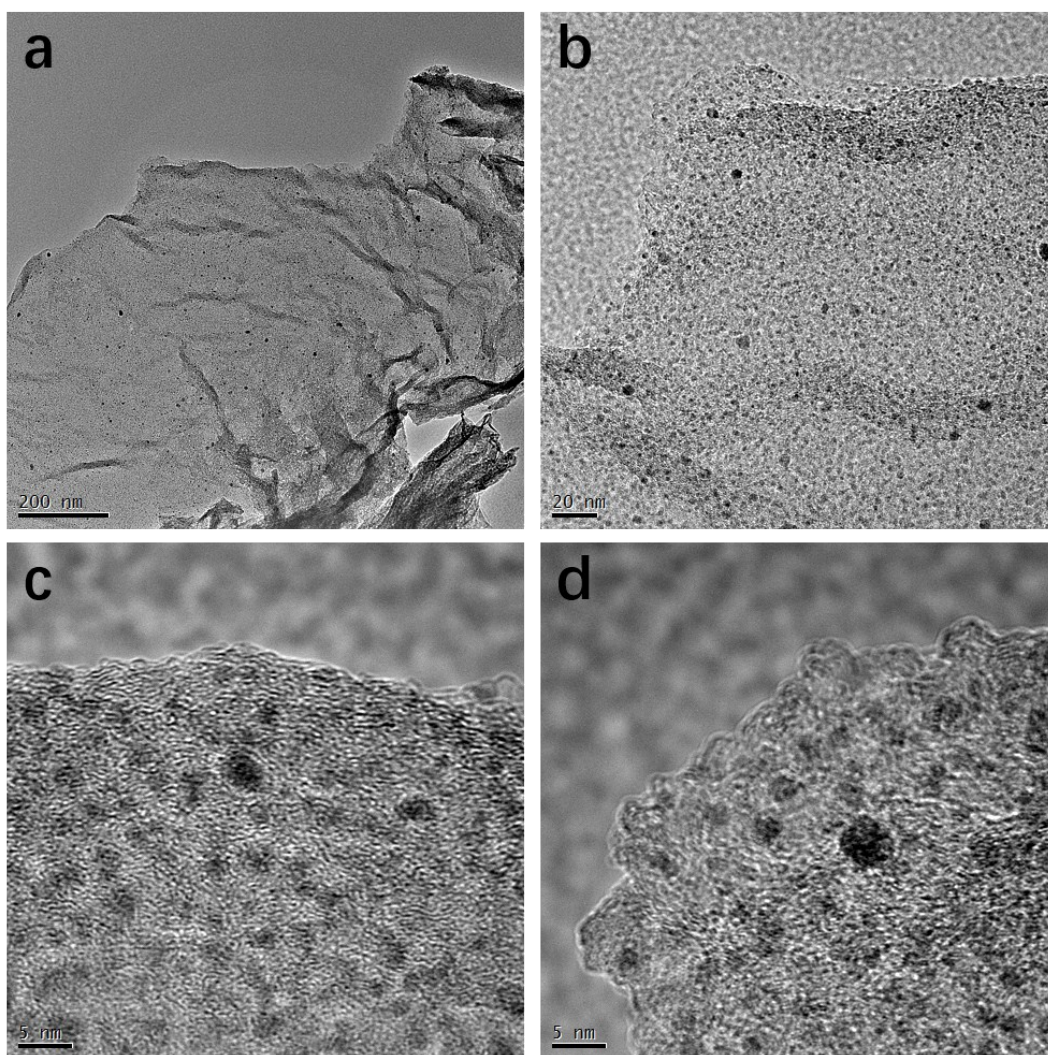


Figure S3. (a-d) TEM images of the Pd/NrGO@SiO₂ catalyst added 1 ml TEOS

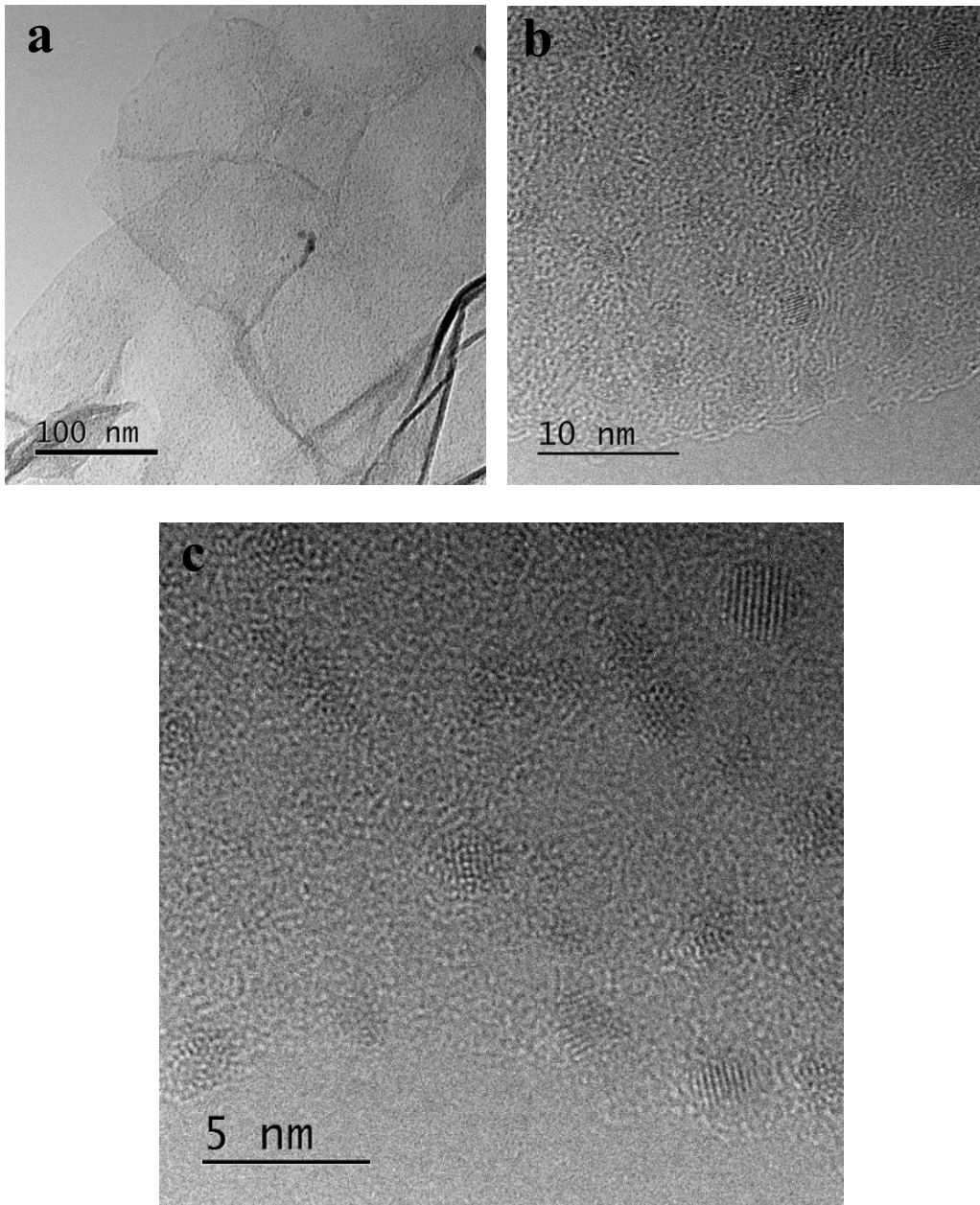


Figure S4. (a), (b) and (c) TEM images of Pd/NrGO sample after 300°C heat treatment.

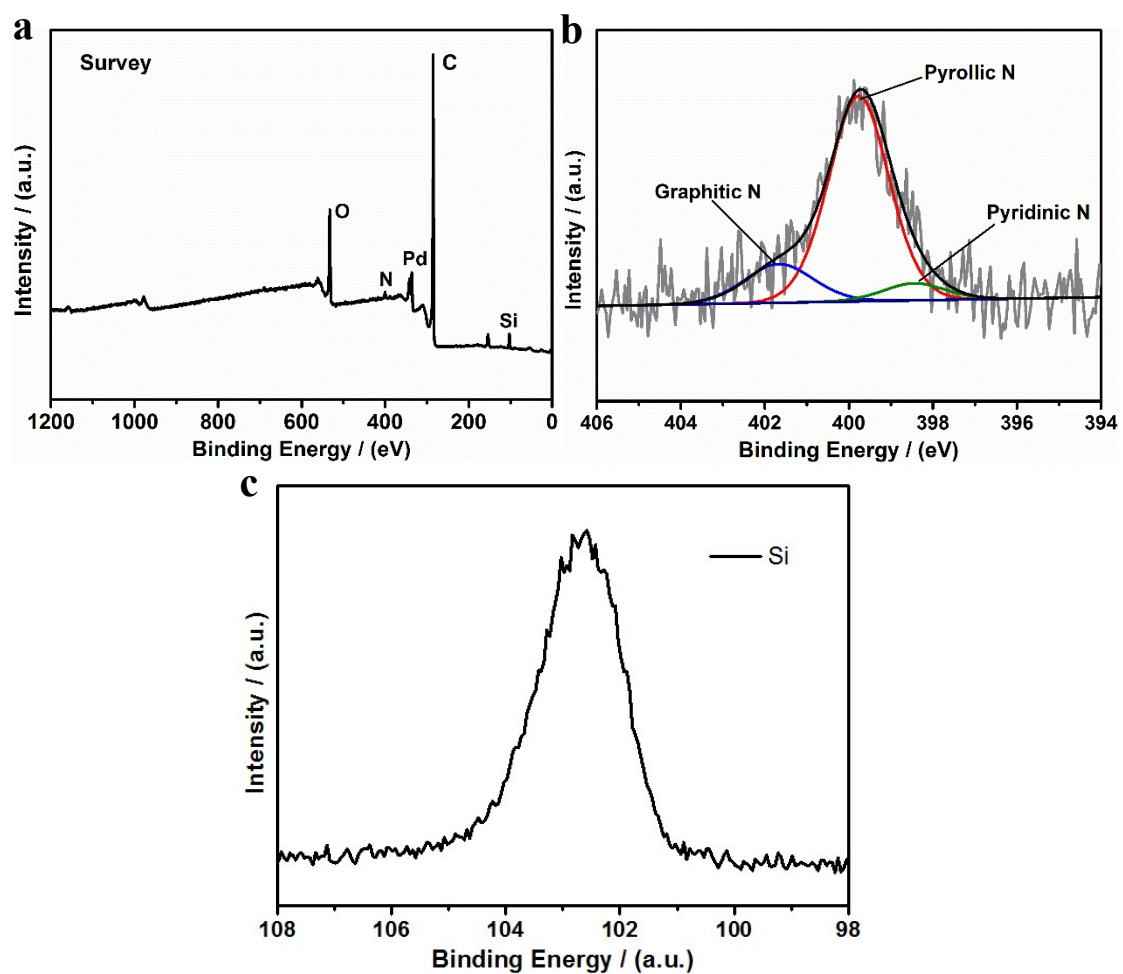


Figure S5. (a) XPS full spectrum (b) N high-resolution spectrum and (c) spectrum of Si element existed in Pd/NrGO@SiO₂ catalyst

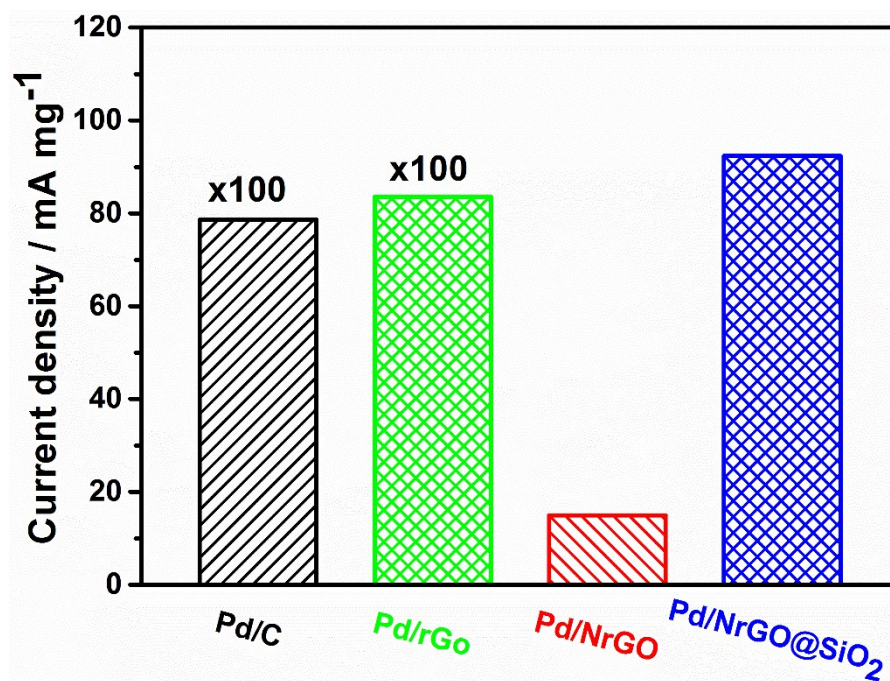


Figure S6. The current density of Pd/NrGO@SiO₂, Pd/NrGO, Pd/rGO and Pd/C in N₂-saturated 0.5 M HCOOH + 0.5 M H₂SO₄ solution after 1 h at 0.05 V vs. Ag/AgCl.

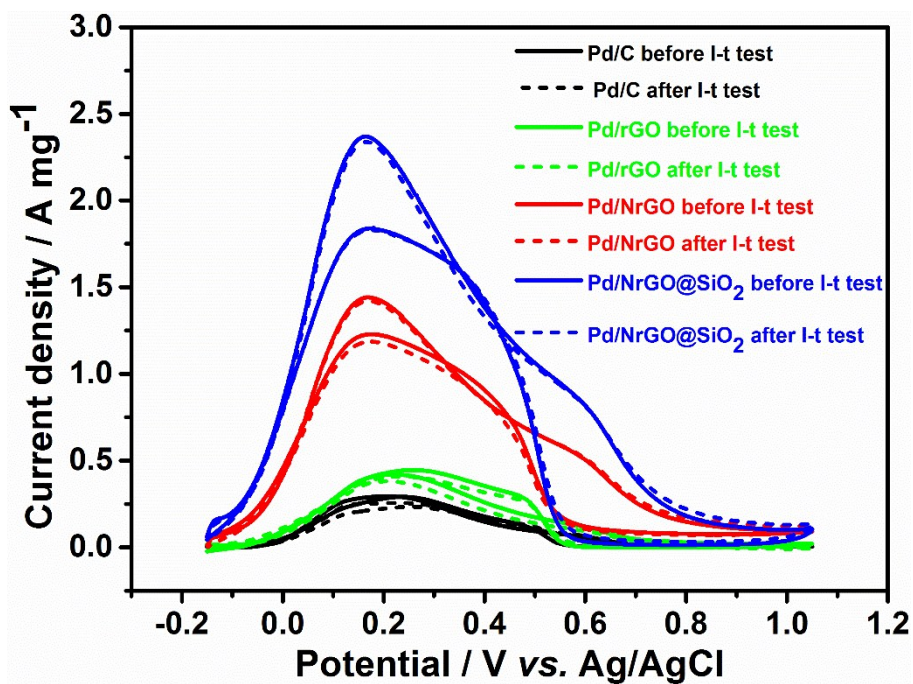
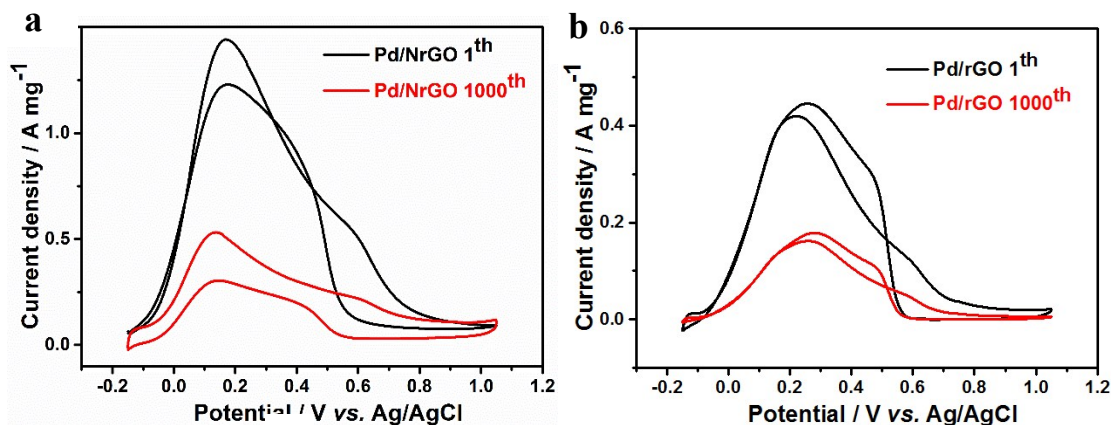
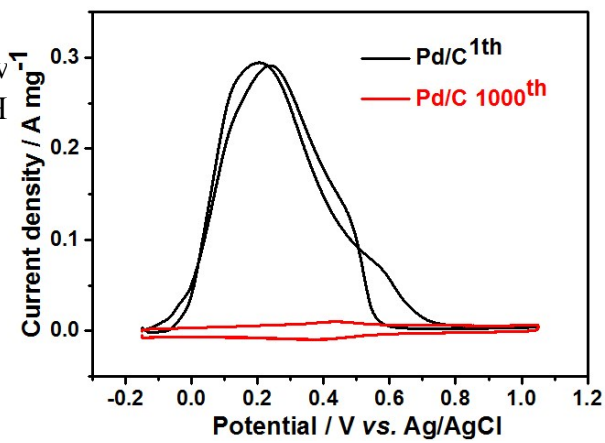


Figure S7. FAOR CV curves of Pd/NrGO@SiO₂, Pd/NrGO, Pd/rGO and Pd/C catalysts before and after 3600s i-t test at 0.05 V vs. Ag/AgCl.



c

Figure S8. CV curv⁻¹
HCOOH + 0.5 M H



N₂-saturated 0.5 M

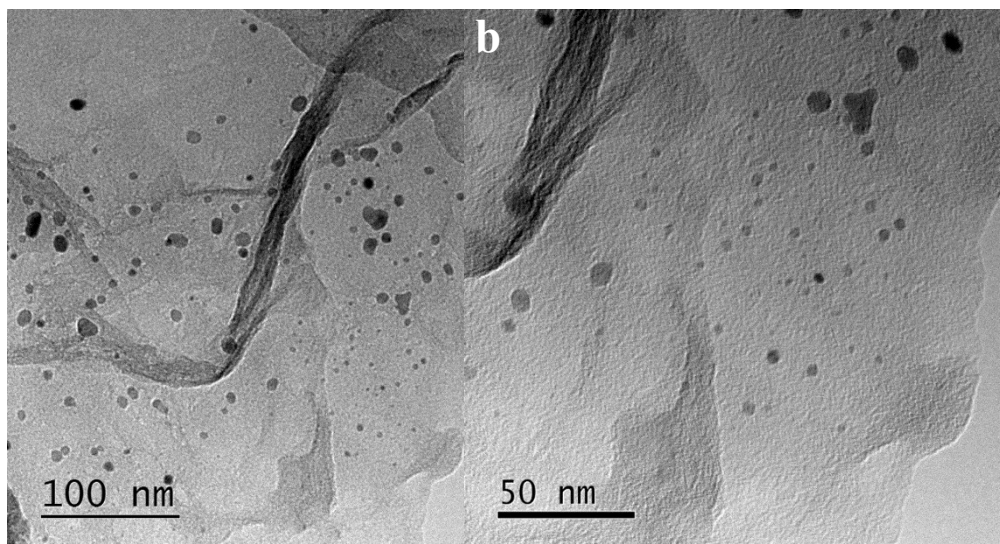


Figure S9. (a) and (b) TEM images after ADT of Pd/NrGO.

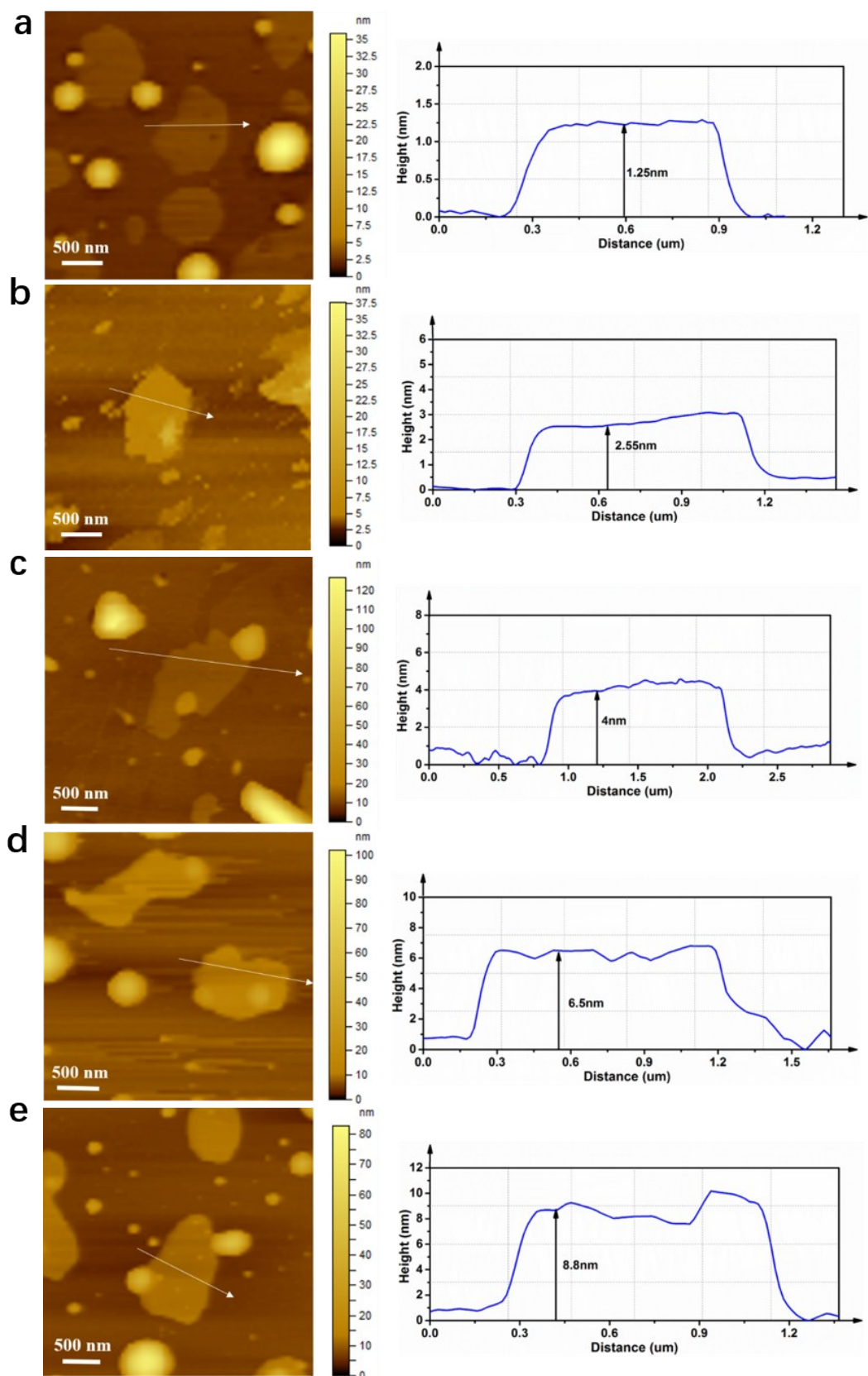


Figure S10. AFM images and corresponding analysis of thicknesses from the line selected in AFM images of (a) Pd/NrGO (b) Pd/NrGO@25ulSiO₂ (c) Pd/NrGO@50ulSiO₂ (d) Pd/NrGO@100ulSiO₂ (e) Pd/NrGO@150ulSiO₂.

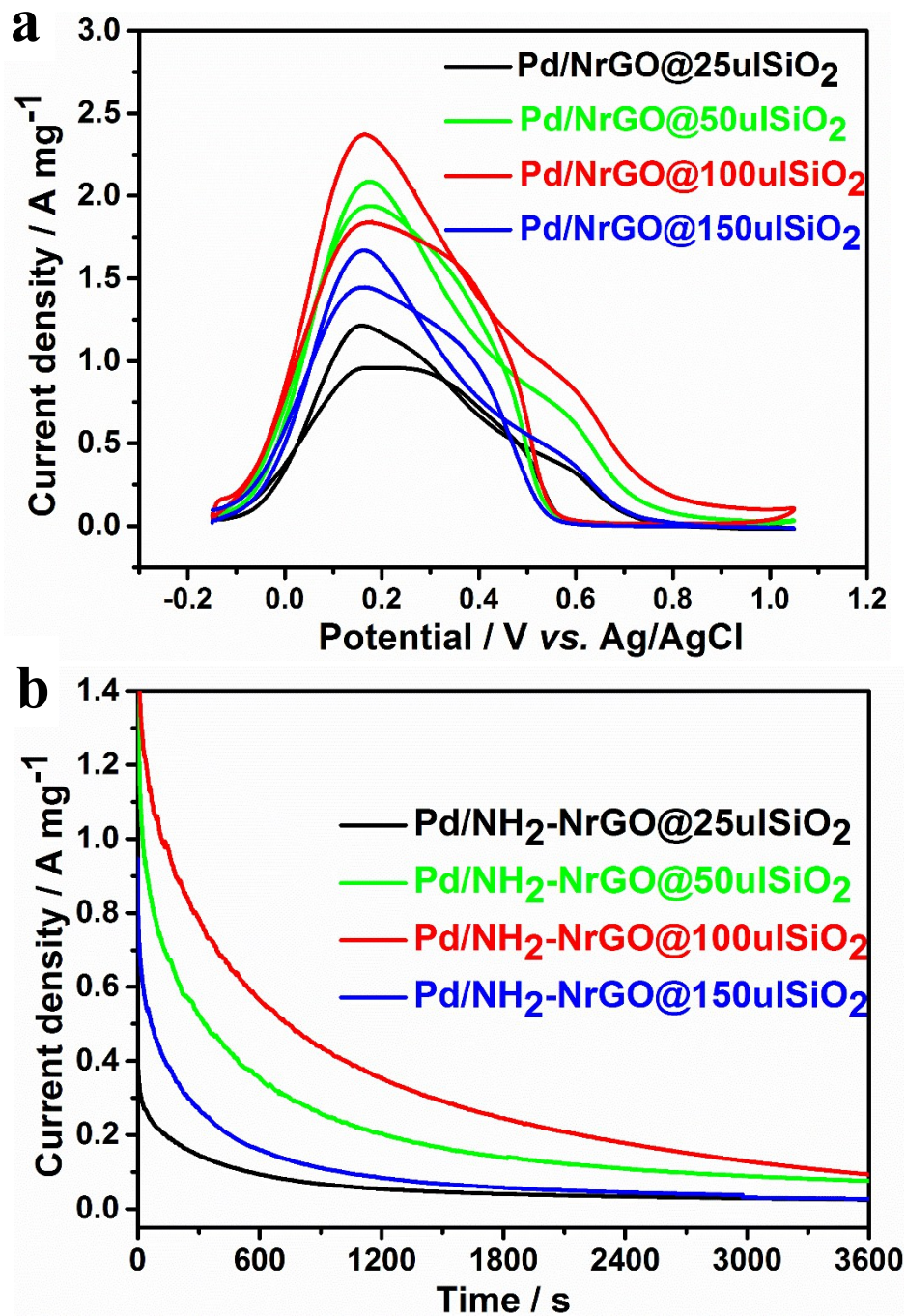


Figure S11. (a) CV curves and (b) *i*-*t* curves at 0.05 V vs. Ag/AgCl for 3600 s of Pd/NrGO@25ulSiO₂, Pd/NrGO@50ulSiO₂, Pd/NrGO@100ulSiO₂, Pd/NrGO@150ulSiO₂ samples in 0.5 M HCOOH + 0.5 M H₂SO₄ solution containing saturated N₂.

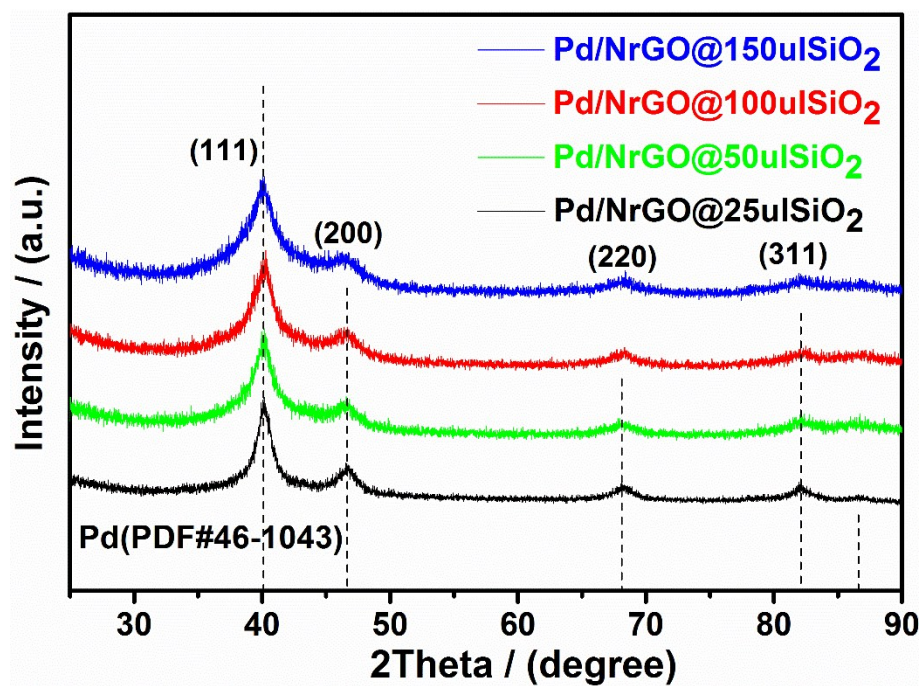


Figure S12. XRD patterns for Pd/NrGO@SiO₂ added different TEOS amounts.

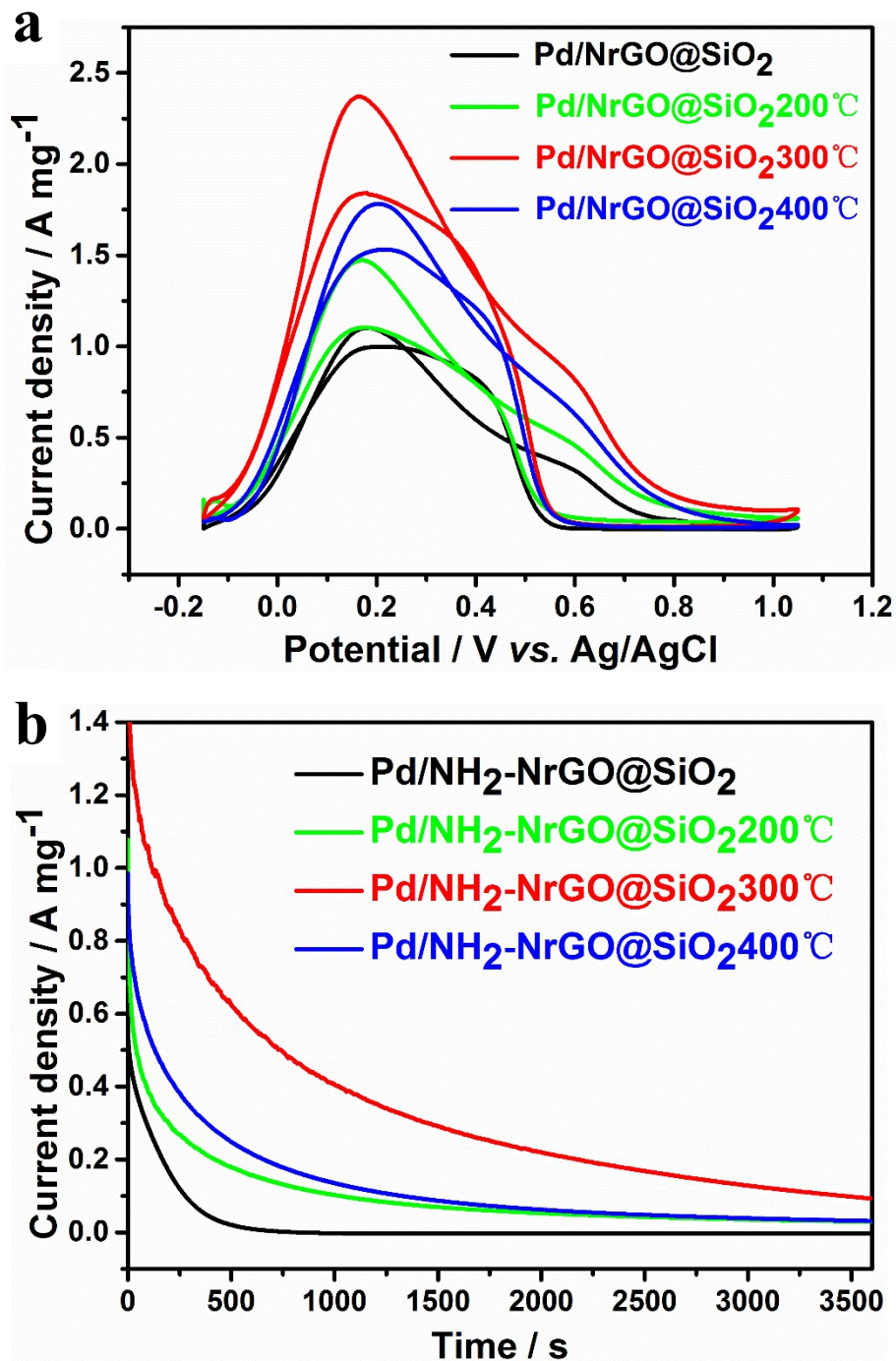
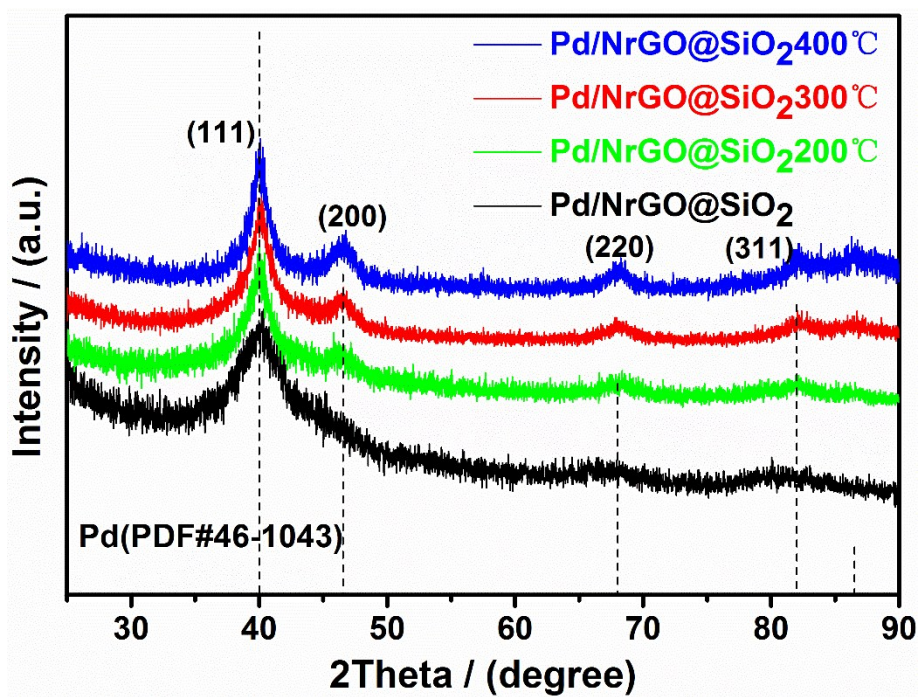


Figure S13. (a) CV curves and (b) *i*-*t* curves at 0.05 V vs. Ag/AgCl for 3600 s of Pd/NrGO@SiO₂ added 100ul TEOS treated at 200°C, 300°C, 400°C samples in 0.5 M HCOOH + 0.5 M H₂SO₄ solution containing saturated N₂.



FigureS14. XRD patterns for Pd/NrGO@SiO₂ added 100ul TEOS without heat treatment and treated at 200°C, 300°C, 400°C.

Table S1. A comparison of the electro-catalytic activity of Pd/NrGO@SiO₂, Pd/NrGO, Pd/rGO and Pd/C catalysts toward formic acid oxidation

catalysts	ECSA [m ² g ⁻¹]	Mass activity (A mg ⁻¹)	Specific activity (mA cm ⁻²)	I _f / I _b
Pd/NrGO@SiO ₂	64.7	2.37	3.7	1.28
Pd/NrGO	37.9	1.44	3.8	1.18
Pd/rGO	19.8	0.42	2.2	1.06
Pd/C	14.5	0.30	2.0	0.97

Table S2. Formic acid oxidation behavior on Pd/NrGO@SiO₂ with those of the recent Pd-based Catalysts reported

Catalysts	Forward peak current density (A mg ⁻¹ Pd)	Formic acid concentration (M)	Electrolyte	References
Pd/NrGO@SiO ₂	2.37	0.5	0.5 M H ₂ SO ₄	This work
Pd/rGO@pSiO ₂	1.125	0.25	0.5 M H ₂ SO ₄	2
Pd/PRGO	1.112	1.0	0.5 M H ₂ SO ₄	3
Pd NF/HPMo-G	1.02	0.5	0.5 M H ₂ SO ₄	4
Pd 2D NFs	0.940	0.5	0.5 M H ₂ SO ₄	5
PdSP@rGO	0.63	0.5	0.5 M H ₂ SO ₄	6
Pd/NP-Coal-CFs (DCD/TPP)	0.5366	0.5	0.5 M H ₂ SO ₄	7
Pd-Mo ₂ N/rGO	0.5327	0.5	0.5 M H ₂ SO ₄	8
2D Porous Pd nanosheets	0.4093	0.5	0.5 M H ₂ SO ₄	9
Pd arrow-headed tripods	0.401	0.5	0.5 M H ₂ SO ₄	10
Pd-DNA@Graphene	0.1401	0.5	0.5 M H ₂ SO ₄	11
Pd@Graphene	0.0895	0.5	0.5 M H ₂ SO ₄	12

Table S3. The stability of Pd/NrGO@SiO₂ catalyst with those of the recent Pd-based Catalysts reported

Catalysts	circles	Remainin g rate / %	Scan rates / mV S ⁻¹	Potential Range / V vs. RHE)	References
Pd/NrGO@SiO ₂	1000	95	100	0.05-1.25	This work
Pd/NS-G	50	58.6	50	0.05-1.25	13
Pd NPs on graphene	250	90	50	0-1.05	14
PdNPs-GO	100	95.6	N.A.	0.05-1.25	15
Pd NF/HPMo-G	100	101.9	N.A.	0.05-1.05	4
Pd/rGO@pSiO ₂	1000	84	100	0.05-1.25	2
Pd nanosheets	1000	57	N.A.	0.05-1.05	9
ordered Pd ₃ Fe/C	1000	85.2	100	0-1.0	16

Reference:

- 1 N. C. Cheng, J. Liu, M. N. Banis, D. S. Geng, R. Y. Li, S. Y. Ye, S. Knights and X. L. Sun, *Int. J. Hydrogen Energy*, 2014, **39**, 15967-15974.
- 2 J. Shan, Z. Lei, W. Wu, Y. Tan, N. Cheng and X. Sun, *ACS Appl. Mater. Interfaces* **2019**, **11**, 43130-43137.
- 3 Y. Zhou, X.-C. Hu, Q. Fan and H.-R. Wen, *J. Mater. Chem. A* 2016, **4**, 4587-4591.
- 4 X. Fan, W. Yuan, D. H. Zhang and C. M. Li, *ACS Appl. Energy Mater.*, 2018, **1**, 411-420.
- 5 Y. Yan, X. Li, M. Tang, H. Zhong, J. Huang, T. Bian, Y. Jiang, Y. Han, H. Zhang and D. Yang, *Adv. science*, 2018, **5**, 1800430.
- 6 Y. Jiang, Y. Yan, W. Chen, Y. Khan, J. Wu, H. Zhang and D. Yang, *Chem. Commun.*, 2016, **52**, 14204-14207.
- 7 M. Lou, R. Wang, J. Zhang, X. Tang, L. Wang, Y. Guo, D. Jia, H. Shi, L. Yang, X. Wang, Z. Sun, T. Wang and Y. Huang, *ACS Appl. Mater. Interfaces*, 2019, **11**, 6431-6441.
- 8 H. Yan, Y. Jiao, A. Wu, C. Tian, L. Wang, X. Zhang and H. Fu, *J. Mater. Chem. A*, 2018, **6**, 7623-7630.
- 9 X. Qiu, H. Zhang, P. Wu, F. Zhang, S. Wei, D. Sun, L. Xu and Y. Tang, *Advanced Functional Materials*, 2017, **27**, 1603852.
- 10 N. Su, X. Chen, Y. Ren, B. Yue, H. Wang, W. Cai and H. He, *Chem. Commun.*, 2015, **51**, 7195-7198.
- 11 F.-Z. Song, Q.-L. Zhu, X. Yang, W.-W. Zhan, P. Pachfule, N. Tsumori and Q. Xu, *Adv. Energy Mater.*, 2018, **8**, 1701416.
- 12 L. Y. Zhang, Z. L. Zhao and C. M. Li, *Nano Energy*, 2015, **11**, 71-77.
- 13 X. Zhang, J. Zhu, C. S. Tiwary, Z. Ma, H. Huang, J. Zhang, Z. Lu, W. Huang and Y. Wu, *ACS Appl. Mater. Interfaces*, 2016, **8**, 10858-10865.
- 14 T. Jin, S. Guo, J.-l. Zuo and S. Sun, *Nanoscale*, 2013, **5**, 160-163.
- 15 X. Chen, G. Wu, J. Chen, X. Chen, Z. Xie and X. Wang, *J. A. Chem. Soc.*, 2011, **133**, 3693-3695.
- 16 Z. Liu, G. Fu, J. Li, Z. Liu, L. Xu, D. Sun and Y. Tang, *Nano Res.*, 2018, **11**, 4686-4696.